

Controllable cascaded four-wave mixing by two chirped femtosecond laser pulses

H. Zhang · Z. Zhou · A. Lin · J. Cheng · H. Liu · J. Si ·
F. Chen · X. Hou

Received: 30 November 2011 / Revised version: 14 March 2012 / Published online: 26 May 2012
© Springer-Verlag 2012

Abstract We investigated the generation of cascaded four-wave mixing (CFWM) sidebands by using two crossing chirped femtosecond pulses with the same central wavelength in tellurite glass (Te glass). Sidebands of broadband spectra, which contained non-degenerate and degenerate CFWM signals, were obtained at different delay time between two input pulses. The CFWM sidebands observed on different sides of input beams were flexibly controlled by adjusting the delay time.

1 Introduction

In this decade, the laser pulse generation of ultra-broadband spectrum and ultrashort duration became a hot research spot [1, 2]. Since the first observation of the non-degenerate cascaded four-wave mixing (CFWM) in femtosecond timescale in BK7 glass [3], the technique of generating wavelength-tunable multicolor ultrashort laser pulses has been well developed. The CFWM signals were generated by using two femtosecond laser pulses with different frequencies inter-

acting in a $\chi^{(3)}$ medium. A small crossing angle between two incident beams was employed to compensate for the phase mismatch which was introduced by the high material dispersion in the solid-state media. These tunable multicolor ultrashort pulses can be used in many fields, such as multicolor pump–probe experiments [4, 5], femtosecond coherent anti-Stokes Raman spectroscopy (CARS) [6, 7].

Recently, broadband CFWM signals have been experimentally generated in sapphire plate [8] and fused silica [9–12]. The frequency up-shifted (down-shifted) CFWM signals appeared on the side of the incident beam with higher (lower) frequency. The sideband spectra could be tuned by changing the crossing angle of the two input beams. However, the incident femtosecond laser pulses used in the previous experiments were pulse-compressed and of different central wavelengths, as less research was done on the state of employing chirped femtosecond laser pulses with the same central wavelength. On the condition of two chirped femtosecond laser pulses with equal central wavelength, the wavelength components interacted in CFWM may be controlled by varying the delay time between two incident pulses. The spectra of CFWM sidebands, which may contain non-degenerate and degenerate components, could be flexibly controlled by adjusting the time delay.

In this paper, we investigate the generation of the laser pulses with broad spectral bandwidth by using two chirped femtosecond laser pulses with the same central wavelength in tellurite glass (Te glass). The generation of CFWM sidebands was flexibly controlled by adjusting the delay time between two input pulses. The sidebands containing non-degenerate and degenerate CFWM signals at different delay times help us to conveniently select the laser pulses with different wavelengths.

H. Zhang · J. Cheng · H. Liu · J. Si (✉) · F. Chen · X. Hou
Key Laboratory for Physical Electronics and Devices
of the Ministry of Education & Shaanxi Key Lab of Information
Photonic Technique, School of Electronic & Information
Engineering, Xi'an Jiaotong University, Xianning-xilu 28,
Xi'an 710049, People's Republic of China
e-mail: jinhaisi@mail.xjtu.edu.cn
Fax: +86-029-82663485

Z. Zhou · A. Lin
State Key Laboratory of Transient Optics and Photonics,
Xi'an Institute of Optics and Precision Mechanics (XIOPM),
Chinese Academy of Sciences (CAS), Xi'an 710119,
People's Republic of China

2 Experiments

The non-resonant type homogeneous Te glass sample with composition $80\text{TeO}_2\text{-}10\text{ZnO-}10\text{Na}_2\text{O}$ was prepared by conventional melt-quenching method. Reagent chemical powders with purity $\geq 99.9\%$ were precisely weighed up, homogeneously mixed in a glass bottle, melted in a golden crucible at about $800\text{ }^\circ\text{C}$ for 1 h, poured onto a brass mold at $220\text{ }^\circ\text{C}$, annealed at $259\text{ }^\circ\text{C}$ for 8 h, and then slowly cooled down to room temperature. The Te glass sample was polished to a 1-mm thickness. The nonlinear refractive index n_2 of the Te glass was measured to be $\sim 10^{-15}\text{ cm}^2/\text{W}$ [13]. The linear transmission spectrum of the Te glass showed that the absorption edge was located at about 380 nm and provided excellent transparency from 0.4 up to $6.1\text{ }\mu\text{m}$ [14].

In the experiments, a femtosecond pump-probe arrangement was employed, as described elsewhere [15]. The multipass amplified Ti:sapphire laser system produced pulses with the pulse duration of 30 fs, a central wavelength of 800 nm, and a repetition rate of 1 kHz. The output beam was split into two relatively delayed parts, beam 1 and beam 2. The two beams were focused onto the Te glass by a lens with the focal length of 300 mm at a small angle of 2.8° . A time-delay device, which was controlled by a computer, was used to adjust the timing of pulse collisions. The delay time Δt between the two pulses was calibrated using the autocorrelation signal from second-harmonic generation (SHG) in a 1-mm-thick BBO crystal. The full width at half maximum (FWHM) of the incident pulse was about 260 fs at the position of the sample. The beam diameters of beam 1 and beam 2 on the sample were both about $300\text{ }\mu\text{m}$, which were measured using knife-edge method. The input power of beam 1 and beam 2 was 8 and 6.5 mW, respectively. In the experiments, no supercontinuum was detected, and the effect of supercontinuum generation on our experimental results could be excluded. The intensity and spectral profile of the signals were detected by a photomultiplier tube (PMT) and an optical multi-channel analyzer (OMA), respectively.

3 Experimental results and discussion

Two femtosecond laser pulses with different wave vectors (\vec{k}_1 , \vec{k}_2 , and $\vec{k}_1 > \vec{k}_2$) interacted in $\chi^{(3)}$ medium at a small angle, the frequency up-shifted CFWM signals appeared on \vec{k}_1 side, and the frequency down-shifted CFWM signals appeared on \vec{k}_2 side. The phase matching condition of the first-order frequency up-shifted CFWM signal (with wave vector $\vec{k}_1^{(+1\text{st})}$) was described by $\vec{k}_1^{(+1\text{st})} = 2\vec{k}_1 - \vec{k}_2$. The higher m th-order frequency up-shifted CFWM signals obeyed the

following off-axis phase match condition [3, 16]: $\vec{k}_1^{(+m\text{th})} = \vec{k}_1^{(m-1)\text{th}} + \vec{k}_1 - \vec{k}_2 \approx (m+1)\vec{k}_1 - m\vec{k}_2$. The first-order frequency down-shifted CFWM signal (with wave vector $\vec{k}_1^{(-1\text{st})}$) was described by $\vec{k}_1^{(-1\text{st})} = 2\vec{k}_2 - \vec{k}_1$. By using the chirped femtosecond laser pulses with the same central wavelength, abundant pairs of (\vec{k}_1 , \vec{k}_2) could be obtained at different delay times between two input pulses. Thus, the CFWM sideband generation can be controlled by adjusting the delay time. In our notation, positive (negative) delay time Δt corresponds to beam 2 (beam 1) preceding beam 1 (beam 2), and $\Delta t = 0$ fs denotes the complete incident pulses overlap. The frequency up-shifted CFWM signals appeared on beam 1 side when the delay time was negative, while on beam 2 side when the delay time was positive.

The background-free time-integrated signal (the total energy) in the direction of the first-order CFWM signal on beam 1 side as a function of the delay time Δt was measured, as shown in Fig. 1(a). The result showed a three-peak structure profile, in which the peaks appeared at the

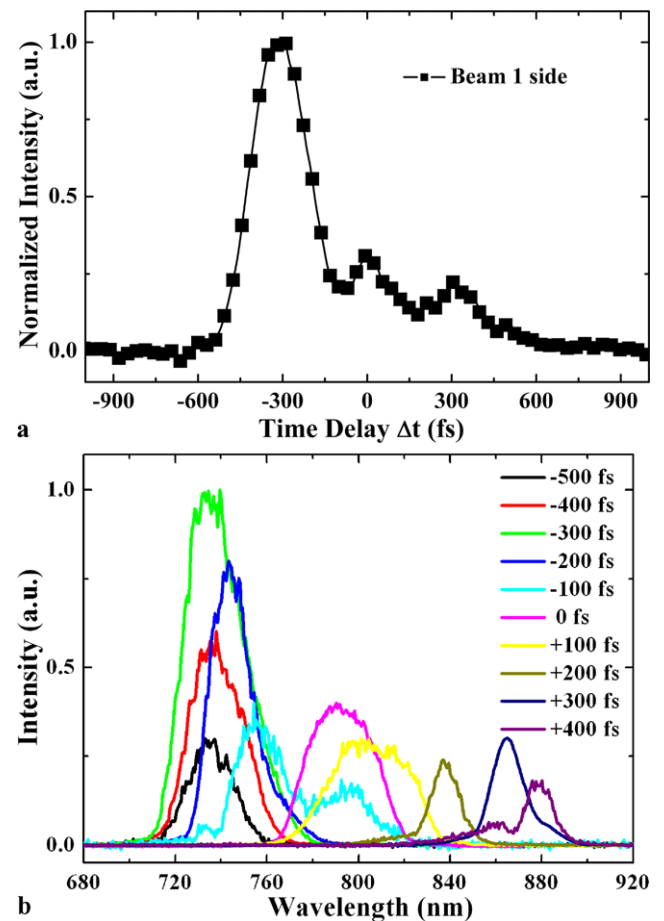


Fig. 1 (a) Dependence of time-integrated signal in the direction of the first-order CFWM signal on the delay time Δt between pulse 1 and pulse 2. (b) The synchronized spectra obtained by varying the delay time

delay time of about $-310, 0,$ and $+310$ fs, respectively. The peaks appearing at -310 and $+310$ fs were attributed to the first-order frequency up-shifted and down-shifted CFWM signals on beam 1 side, respectively. The peak around 0 fs was attributed to the generation of the first-order degenerate CFWM signal on beam 1 side. The dominant mechanism and characterization of the sideband generation at the three delay times will be described below.

Figure 1(b) shows the synchronized spectra by varying the delay time. The central wavelength moves from about 730 to 880 nm as the delay time is varying from -500 to $+400$ fs. When the delay time of two incident pulses was larger than 200 fs, the obtained signals were the non-degenerate CFWM signals, whose spectra were out of the range of incident pulses. When the delay time was smaller than 200 fs, the degenerate processes became the dominant mechanism to generate the sideband signals. The spectra of degenerate CFWM signals were around 800 nm, which was the central wavelength of the incident pulses. By employing the non-degenerate and degenerate CFWM, the spectral tuning range extended from 710 to 890 nm in this direction. It would be expected that the non-degenerate and degenerate CFWM signals would also be obtained in the direction of the first-order signal on beam 2 side.

Figure 2(a) shows the photograph of the sideband signals, in which the delay time between two incident pulses

was $\Delta t = -310$ fs. Seven spots were simultaneously observed on beam 1 side (denoted as L1–L7) and one spot was observed on beam 2 side (denoted as L-1). L1–L7 were frequency up-shifted CFWM signals and L-1 was a frequency down-shifted CFWM signal. The wavelengths of the CFWM signals are shown in Fig. 2(b), in which we can see that the higher order signal on beam 1 side has a shorter central wavelength. The transmitted differential spectra of beam 1 and beam 2 are also shown in Fig. 2(b), which are the differences between the transmitted spectra of one incident beam (beam 1 or beam 2) with and without the other incident beam (beam 2 or beam 1). A valley at 776 nm for beam 1 and another valley at 818 nm for beam 2 are observed, manifesting that the corresponding central wavelengths of \vec{k}_1 and \vec{k}_2 were located at 776 and 809 nm, respectively. The central wavelength of L-1 ($k_1^{(-1st)}$) was 852 nm.

When the delay time between two incident pulses was positive, the frequency up-shifted CFWM signals were observed on beam 2 side, while the frequency down-shifted CFWM signal appeared on beam 1 side. Figure 3(a) shows the photograph of CFWM signals, which was taken at the delay time of $+310$ fs. The spectra of the sideband and the transmitted differential spectra of beam 1 and beam 2 are shown in Fig. 3(b). The central wavelengths of primary interacting pairs (\vec{k}_1', \vec{k}_2') for this time scale were 829

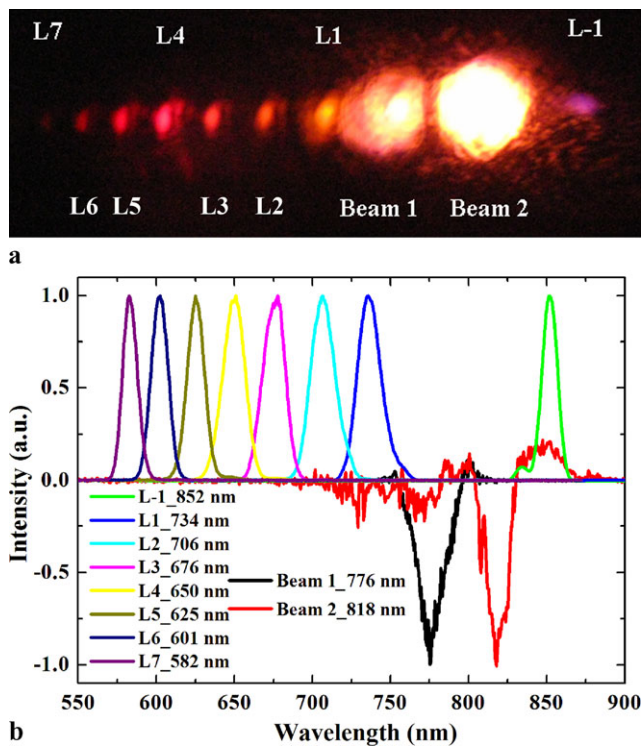


Fig. 2 (a) Photograph of CFWM signals at the delay time $\Delta t = -310$ fs. (b) Normalized spectra of the sideband signals of L1–L7 on beam 1 side, L-1 on beam 2 side, and transmitted differential spectra of beam 1 and beam 2

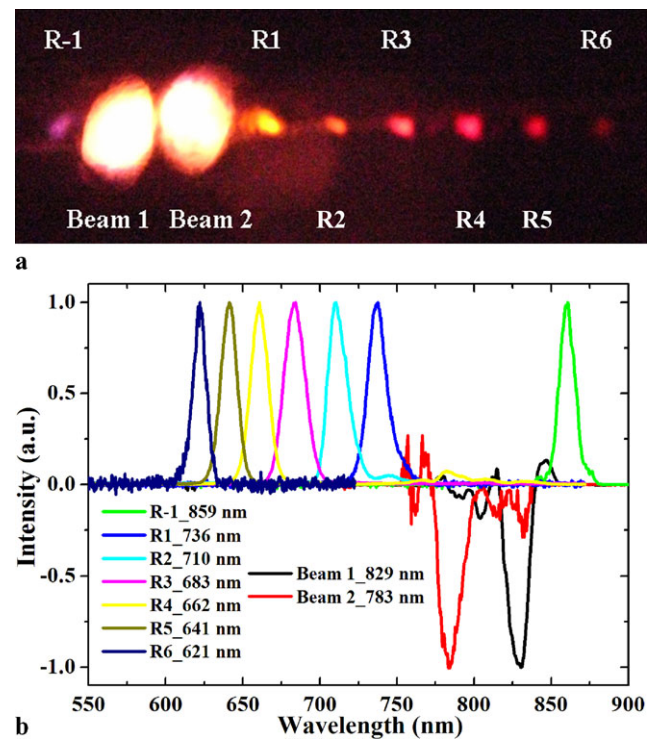


Fig. 3 (a) Photograph of CFWM signals at the delay time $\Delta t = +310$ fs. (b) Normalized spectra of the sideband signals of R1–R6 on beam 2 side, R-1 on beam 1 side, and transmitted differential spectra of beam 1 and beam 2

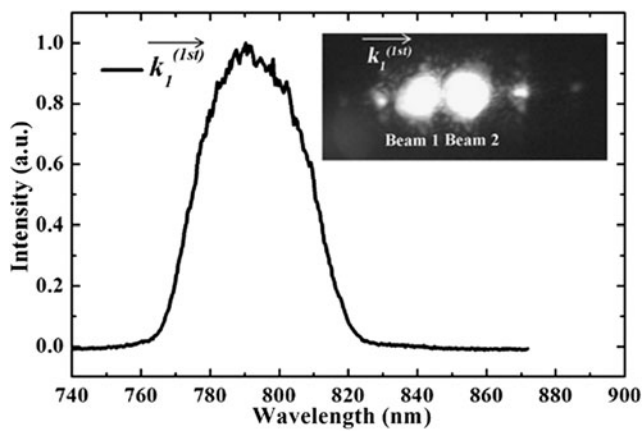


Fig. 4 Spectrum of the first-order degenerate CFWM signal ($\vec{k}_1^{(1st)}$) on beam 1 side. The inset shows the photograph of degenerate CFWM signals. The delay time Δt between two incident pulses was 0 fs

and 783 nm, which were different from that at a negative delay time of -310 fs. Therefore, the spectra of frequency up-shifted signals obtained at $+310$ fs (R-series) were different from those obtained at -310 fs (L-series). On beam 1 side, the first-order frequency down-shifted CFWM signal was observed and its central wavelength was 859 nm.

There were much more frequency up-shifted CFWM signals than the frequency down-shifted signals at the two measured delay times. The asymmetric pattern on two sides was limited by the asymmetric phase mismatch condition [3]. The overall energy conversion efficiency from the incident beams to the sidebands reached more than 5 %.

When the two incident laser pulses with the same wavelengths overlapped temporally and spatially in the Te glass, the degenerate CFWM processes became the dominated mechanism to generate the sideband signals, which can be called self-diffraction signals [17–22]. Figure 4 shows the spectrum of the first-order degenerate CFWM signal ($\vec{k}_1^{(1st)}$) on beam 1 side. The central wavelength of $\vec{k}_1^{(1st)}$ was located at 795 nm with FWHM of 35 nm. When the degenerate CFWM process was generated by off-axis pumps, the wave vector of the first-order degenerate CFWM signal was given by $|\vec{k}| \times \sqrt{[1 + 4 \times (1 - \cos \theta)]}$, where $|\vec{k}|$ was the amplitude of both pumps (with the same wavelengths) and θ was the angle between the two crossing pumps. The central wavelength blue-shift of the first-order degenerate CFWM signal was observed. The inset of Fig. 4 shows the photograph of degenerate CFWM signals taken at the delay time of 0 fs. We can see that two spots appeared on both sides of incident beams. The distribution of degenerate CFWM signals presented symmetric pattern, which was different from that of non-degenerate CFWM condition.

Wavelength-tunable laser pulses with broad-bandwidth were generated by using two chirped femtosecond laser

pulses with same central wavelength in Te glass. Wide spectral tuning range was obtained in the direction of the first-order degenerate CFWM signal by controlling the delay time between two incident pulses. The generation of CFWM sideband was flexibly controlled by adjusting the delay time. The frequency up-shifted laser pulses appeared on beam 1 (beam 2) side when the delay time was negative (positive). The multicolor sidebands may be used in many fields, such as multicolor pump–probe experiments.

4 Conclusion

We investigated the generation of wavelength-tunable laser pulses with broad-bandwidth by using two chirped femtosecond laser pulses with same central wavelength in Te glass. Non-degenerate and degenerate CFWM signals were obtained in the same direction at different delay times. The CFWM sideband generation was flexibly controlled by adjusting the delay time between two incident pulses.

Acknowledgements The authors gratefully acknowledge the financial support for this work provided by the National Science Foundation of China under the Grant No. 91123028, the National Basic Research Program of China (973 Program) under the Grant No. 2012CB921804, and the National Science Foundation of China under the Grant Nos. 11074197 and 60907039, and the West Light Foundation from the Chinese Academy of Sciences.

References

1. F. Théberge, N. Aközbeke, W. Liu, A. Becker, S.L. Chin, *Phys. Rev. Lett.* **97**, 023904 (2006)
2. T. Fuji, T. Suzuki, *Opt. Lett.* **32**, 3330 (2007)
3. H. Crespo, J.T. Mendonça, A. Dos Santos, *Opt. Lett.* **25**, 829 (2000)
4. T. Kobayashi, A. Shirakawa, T. Fuji, *IEEE J. Sel. Top. Quantum Electron.* **7**, 525 (2001)
5. A. Baltuška, T. Fuji, T. Kobayashi, *Opt. Lett.* **27**, 306 (2002)
6. D. Pestov, R.K. Murawski, G.O. Ariunbold, X. Wang, M.C. Zhi, A.V. Sokolov, V.A. Sautenkov, Y.V. Rostovtsev, A. Dogariu, Y. Huang, M.O. Scully, *Science* **316**, 265 (2007)
7. Y.J. Lee, M.T. Cicerone, *Appl. Phys. Lett.* **92**, 041108 (2008)
8. J. Liu, T. Kobayashi, *Opt. Express* **16**, 22119 (2008)
9. J. Liu, T. Kobayashi, *Opt. Express* **17**, 4984 (2009)
10. J. Liu, T. Kobayashi, *Opt. Lett.* **34**, 1066 (2009)
11. J.L. Silva, R. Weigand, H.M. Crespo, *Opt. Lett.* **34**, 2489 (2009)
12. R. Weigand, J.T. Mendonça, H.M. Crespo, *Phys. Rev. A* **79**, 063838 (2009)
13. R.F. Souza, M.A.R.C. Alencar, J.M. Hickmann, R. Kobayashi, L.R.P. Kassab, *Appl. Phys. Lett.* **89**, 171917 (2006)
14. A. Lin, A. Zhang, E.J. Bushong, J. Toulouse, *Opt. Express* **17**, 16716 (2009)
15. H. Zhang, H. Liu, J. Si, W. Yi, F. Chen, X. Hou, *Opt. Express* **19**, 12039 (2011)
16. J. Liu, T. Kobayashi, *Opt. Commun.* **283**, 1114 (2010)

17. Y.R. Shen, *The Principles of Nonlinear Optics* (Wiley, New York, 1984)
18. H.J. Eichler, P. Günter, D.W. Pohl, *Laser Induced Gratings* (Springer, Berlin, New York, Heidelberg, 1986)
19. T. Schneider, D. Wolfframm, R. Mitzner, J. Reif, *Appl. Phys. B* (1999). doi:[10.1007/s003400050698](https://doi.org/10.1007/s003400050698)
20. J. Reif, R.P. Schmid, T. Schneider, *Appl. Phys. B* (2002). doi:[10.1007/s003400200847](https://doi.org/10.1007/s003400200847)
21. T. Schneider, J. Reif, *Phys. Rev. A* **65**, 023801 (2002)
22. J. Liu, K. Okamura, Y. Kida, T. Kobayashi, *Opt. Express* **18**, 22245 (2010)